



# In Situ Test and Numerical Analysis of Traffic-Load-Induced Cumulative Settlement of Alluvial Silt After Treatment with Burnt Lime

Qing Jin<sup>1</sup>; Xin-zhuang Cui<sup>2</sup>; Jun Li<sup>3</sup>; Jun-wei Su<sup>4</sup>; and Yi-lin Wang<sup>5</sup>

**Abstract:** Alluvial silt is widely distributed in the Yellow River basin, especially in its largest alluvial plain, the Yellow River delta. In this area, owing to the wet and soft characteristics of the alluvial silt, cumulative settlement often occurs under traffic loads. To reduce the settlement, various methods are applied to improve the subgrade bearing capacity in this area. Among them, the use of calcium oxide (burnt lime) to treat shallow subsoil is a common selection. However, the effect and mechanism of this method have not been fully determined. Therefore, a large integrated device was developed for an in situ test so that the comparative analysis of the short-term settlement of the natural and burnt-lime-treated ground under traffic loads can be achieved. For the long-term cumulative settlement, a numerical method using a cumulative deformation model was applied to analyze the settlements after 10 years. Furthermore, the numerical method respectively predicted the settlement after 1 and 2 years to compare with the in situ test. The in situ test results demonstrate that the wave impedance of the alluvial silt subsoil treated with burnt lime grows and both the dynamic stress caused by wheel load and the excess pore water pressure are reduced. These indicated that the short-term cumulative settlement was significantly reduced after the alluvial silt subsoil was treated with burnt lime. Moreover, the results obtained by the numerical method are similar to those in the in situ test. For the long-term cumulative settlement, the calculation results of the numerical method indicated that the use of burnt lime to treat the ground is effective. In detail, 10 years later, the settlement of the burnt-lime-treated ground decreased by about 1/5. DOI: 10.1061/(ASCE)GM.1943-5622.0001571. © 2019 American Society of Civil Engineers.

**Author keywords:** Alluvial silt; Burnt lime treatment; Settlement; In situ test; Numerical calculations.

## Introduction

*Alluvium* is a term used to describe a collection of soil layers composed of fine particles of silt and clay, larger particles of sand and gravel, and other impurity particles. Generally, alluvium is formed as a result of water scouring and remodeling. The soil that makes up the alluvium is called alluvial silt. In China, affected by the Yellow River, alluvial silt is widely distributed along its coast, forming many alluvial plains. Among them, the Yellow River delta is the youngest and largest one. Basically, the alluvial silt rich in the delta is mainly low liquid limit soil. The alluvial soil has terrible engineering properties, such as low liquid limit, low plasticity index, low cohesion, and intensive capillarity. Moreover, alluvial soil has great liquefaction potential and the groundwater level in the Yellow River delta is very high. Therefore, the cumulative settlement caused

by traffic load can lead to serious pavement diseases and even disasters in this region.

More specifically, the excessive settlement will cause the pavement structural layer to reach the material strength limit, accelerate the damage of the road surface, and shorten the service life of the road. Due to the uneven distribution of traffic loads in time and space, this cumulative settlement is also uneven. This will lead to a large change in the cross slope of the subgrade, which will bring safety problems to driving and will cause the water accumulation on the road surface to be more serious, resulting in a series of problems such as road water damage. However, in the Yellow River delta region, it is impossible to not use alluvial silt as an embankment construction material for various reasons.

For such situations, the burnt lime cushion method is mainly used to diminish the cumulative settlement and enhance the bearing capacity of alluvium subsoil in this region. This method is proven to be feasible to improve the bearing capacity of soft wet subsoil (Kamon 1992; Chen and Yu 2011; Heidaripناه et al. 2016; Shankar et al. 2018; Zhou et al. 2018). However, the effect of burnt lime treatment on traffic-load-caused cumulative settlement has not been fully determined.

The existing research on cumulative settlement was mainly based on laboratory tests of dynamic deformation and its numerical simulation. In the 1950s, road settlement under cyclic load was studied by Seed et al. (1955) and Seed and McNeill (1956) through normal compression tests. The features of permanent deformation of subsoil under repeated load were investigated by Monismith et al. (1975) through the repeated-load triaxial compression test. Consolidation settlements of soft clay were studied by Yıldırım and Erşan (2007) through the undrained cyclic simple shear test. Time-dependent settlements affected by destructuration of soft clay

<sup>1</sup>Lecturer, School of Civil Engineering, Shandong Univ., Jinan 250061, PR China. Email: 827762282@qq.com

<sup>2</sup>Professor, School of Civil Engineering, Shandong Univ., Jinan 250061, PR China (corresponding author). ORCID: <https://orcid.org/0000-0003-1501-3931>. Email: cuixz@sdu.edu.cn

<sup>3</sup>Ph.D. Candidate, School of Civil Engineering, Shandong Univ., Jinan 250061, PR China. Email: forzaapis@126.com

<sup>4</sup>Graduate Student, School of Civil Engineering, Shandong Univ., Jinan 250061, PR China. Email: 1571201036@qq.com

<sup>5</sup>Ph.D. Candidate, School of Civil Engineering, Shandong Univ., Jinan 250061, PR China. Email: eason\_wyl@163.com

Note. This manuscript was submitted on November 19, 2018; approved on July 11, 2019; published online on December 11, 2019. Discussion period open until May 11, 2020; separate discussions must be submitted for individual papers. This paper is part of the *International Journal of Geomechanics*, © ASCE, ISSN 1532-3641.

were studied by Nash and Brown (2013) through comparing several elastic viscoplastic models.

A numerical model of consolidation settlement of road embankment in the Yellow River delta was proposed by Zhang et al. (2015). Chai and Miura (2002) analyzed the permanent settlement of a low embankment road with soft subsoil using the modified Li-Selig model (Li and Selig 1996). Lu et al. (2018) calculated the cumulative settlement caused by traffic loads of a low embankment road with soft subsoil through numerous laboratory triaxial tests. Zhuang and Cui (2015) proposed a model to analyze the cumulative settlement induced by repeated traffic loads in the subsoil of a soft soil embankment. Wei et al. (2016) predicted the subsoil deformation of a low embankment road under traffic loads through a new method based on the layerwise summation procedure. The results of Fujiwara et al. (1985) and Fujiwara and Ue (1990) showed that the cumulative settlement of clay under cyclic loads is related to the soil overconsolidation ratio, degree of consolidation at the time of unloading, static loading magnitude, and repeated loading magnitude. However, currently there has been no study on the cumulative settlement of burnt-lime-treated subsoil.

Limited by stress and boundary conditions, laboratory tests can only analyze the traffic-load-induced cumulative sedimentation

under simple conditions. The numerical simulation method can handle the settlement problem with more complicated stress conditions. However, it also has the disadvantages of long calculation time and uncontrollable accumulated calculation errors, which limit its practical use in engineering. Moreover, in actual engineering, the cumulative settlement is caused by the traffic load and the weight of subgrade. It is hard to analyze them separately. Therefore, in situ experiments are an ideal method to simulate settlement caused by traffic loads. In this study, the short-term traffic-load-induced cumulative settlement of alluvial silt subsoil treated by burnt lime was studied through the in situ test and a device called the falling-weight traffic load simulation equipment (FWTLE) was developed for this in situ test. Furthermore, the long-term cumulative settlement was analyzed by the numerical method. Finally, the feasibility of the quicklime treatment method was proven by comparing the difference between the cumulative settlement of the natural ground and that with burnt-lime-treated ground.

## In Situ Tests

### Field of the In Situ Test

The field of the in situ test was selected on Xinzhuangzi Road (Shouguang County, Weifang City, Shandong Province) in the Yellow River delta. The topsoil of the field is the low liquid limit Yellow River alluvial silt. Table 1 provides its main parameters. The groundwater level is 0.6 m from the surface of the in situ test field. The alluvial silt has a low cohesion and a strong tendency to be liquefied. Furthermore, due to the strong capillary phenomenon of the silt, the average saturation of the surface is close to 78%. The grading curve of the alluvial silt has a curvature coefficient exceeding 3. This indicates that its gradation is poorly graded. X-ray diffraction analysis indicated that 80% were nonclay

**Table 1.** Geomechanical parameters of natural subgrade

Topsoil	LL (%)	PI (%)	$W_c$ (%)	$V_r$ (%)	$S_r$ (%)	$C$ (kPa)	$\Phi$ (degrees)	$E_s$ (MPa)
$\leq 0.6$ m	25	7.4	17.6	60.2	0.78	31.8	22.9	7.45
0.6–10 m	27	9.8	18.0	60.3	1.00	26.6	20.5	15.86

Note: LL = liquid limit; PI = plasticity index;  $W_c$  = water content;  $V_r$  = void ratio;  $S_r$  = saturation;  $C$  = cohesion;  $\phi$  = internal friction angle; and  $E_s$  = compression modulus.

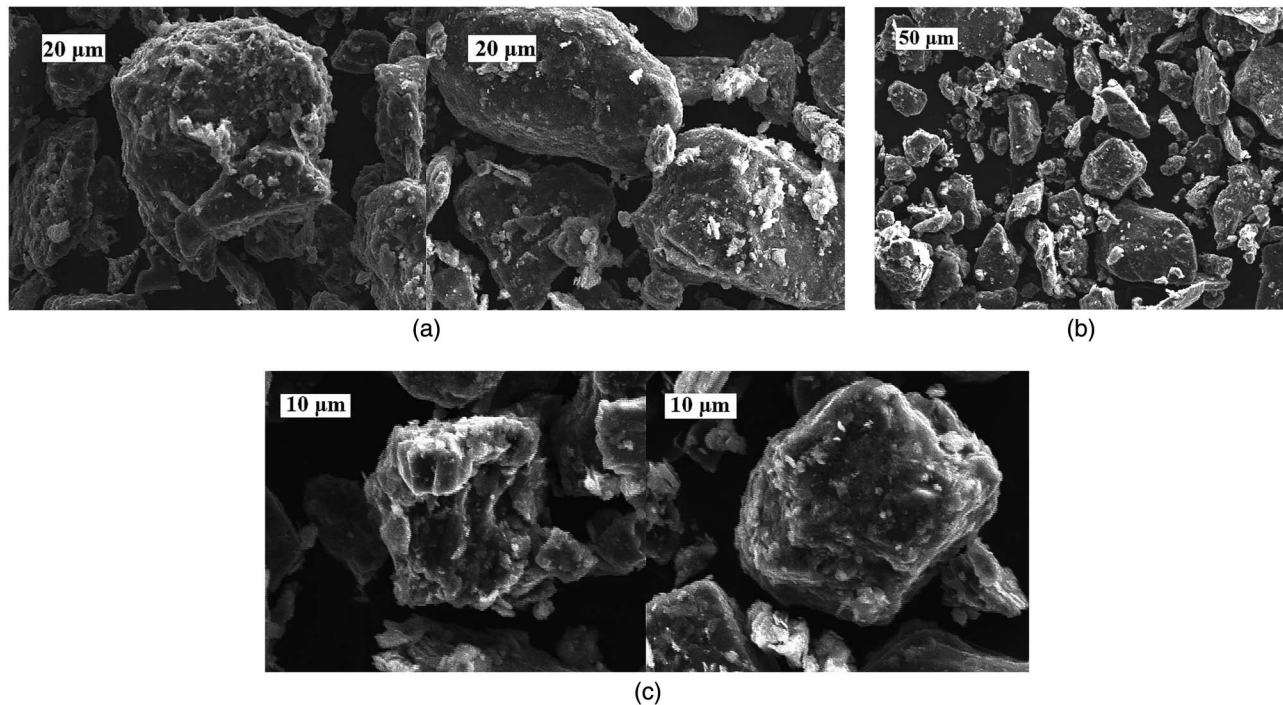


**Fig. 1.** Microstructure of silt: (a) higher sphericity (2,000 $\times$ ); (b) less slender and flaky particles (1,000 $\times$ ); and (c) eroded and destroyed surface (4,000 $\times$ ).

minerals. The microstructure of the particles is shown in Fig. 1, and it was detected by a JXA-8800R (Japan Electronics, Hong Kong) electronic probe. Fig. 1 shows the microstructure of low liquid limit Yellow River delta alluvial silt. It can be seen that the alluvial silt particles in the Yellow River delta have higher sphericity [Fig. 1(a)] and less slender and flaky particles [Fig. 1(b)]. The alluvial silt particles are soaked and scoured in water, colliding with each other, so the surface is severely eroded and destroyed [Fig. 1(c)]. Therefore, it is not easy to be compacted.

According to the design, the soil containing 6% burnt lime was used to treat the 60-cm-thick unsaturated topsoil to achieve the purpose of enhancing the bearing capacity and decreasing the cumulative settlement. Table 2 gives the physical parameters of the burnt-lime-treated soil.

### Device and Parameter Settings of the In Situ Test

The device, FWTLE, was specially developed for this in situ test. It can be used to simulate the action of wheel load on the subsoil for analyzing the cumulative settlement of natural ground (Cui 2012). As shown in Fig. 2, the FWTLE consists of three main systems: automatic control system, pneumatic system, and loading system.

The parameter (e.g., weight and height of falling weight, the stiffness of air spring, and the size of loading plate) setting of FWTLE has a great influence on the simulated results of the in situ test of cumulative settlement. Different parameter settings result in different stress responses of the subsoil. The vertical stress on the ground surface caused by traffic loads has a strong correlation with the height of the road embankment. Previous research indicated that a 100-kN standard-axle load vehicle would produce a 22-kPa vertical stress on the ground surface of a common highway pavement structure (the thickness is approximately 70 cm) and a zero-fill

embankment (the height of the embankment is 0 m) (Cui 2012). However, when the embankment height jumps to 0.8 and 1.5 m, the vertical stress of common highway pavement reduces by 65% and the vertical stress of zero-fill embankment reduces by 75%. Simultaneously, for zero-fill embankment, when the wheel center distance exceeds 0.7 m, the vertical stress slowly changes with the horizontal distance, and this is basically independent of the action time of the wheel load (i.e., vehicle speed).

Therefore, a square loading plate with the size of  $1,200 \times 1,200 \times 3$  mm was used in the situ test. It is equivalent to the area of a circle with a radius of 0.68 m, so it can meet the test accuracy requirements in the case of zero-fill embankments. The hammer (62.5 kg) in the standard penetration test (SPT in geological survey) was used as the drop weight in the test. Due to the large cumulative settlement of the zero-fill embankment, this test adjusts the drop distance.

### Layout of Sensors

The subsoil settlement was monitored by laser displacement sensors in this in situ test. As shown in Fig. 3(a), four feature positions were selected between the loading plate and the subsoil surface for measuring the pressure at the bottom of the plate, where dynamic soil pressure sensors were installed. Fig. 3(b) shows the positions of the dynamic pore pressure sensors and the dynamic soil pressure sensors: Two dynamic pore pressure sensors were respectively installed at 700 and 1,200 mm below the center of the load plate for measuring the dynamic pore pressure in the soil, and two dynamic soil pressure sensors were respectively installed at 600 and 1,000 mm for measuring the dynamic soil pressure in the soil.

## Results and Discussions

### Dynamic Stress

Fig. 4 demonstrates the vertical stress variations of the subsoil surface under the center of the loading plate. The drop distance of weight was 10 cm during the test. Fig. 4(a) indicates that the time histories of stress response are consistent with the factual vertical dynamic stress response of the natural ground surface under a vehicle load (Wang 2007). For natural subsoil, the tested vertical stress on the ground was 23 kPa. As previously described, for the common pavement structure model the vertical stress on the ground surface under the zero-fill embankment was 22 kPa. The tested stress was not much different from the calculated one. Moreover, the single loading period of the dynamic stress (corresponding to a drop-weight height of 10 cm) was 0.031 s. It was roughly equivalent to a vehicle speed of 120 km/h (Huang 1993). Therefore, at the drop-weight height of 10 cm, the FWTLE simulates the stress on the road with zero-fill embankment caused by a vehicle speed of 120 km/h. It can be seen from Fig. 4(b) that the stress on the subsoil surface after the burnt lime treatment increases. This is because a series of chemical reactions occur during the mixing process of the soft wet soil and the burnt lime: water absorption, exothermic reaction, expansion reaction, ion exchange action, carbonation (chemical cementation reaction), pozzolanic reaction (chemical gelation reaction), and crystallization reaction. After these reactions, the moisture in the soil reduced and the slit particles formed a larger aggregate. This makes the soil particles bond together and gradually harden so that the physical and mechanical properties of the subsoil are enhanced.

The variation trends of vertical stress amplitude of the subsoil under the center of the loading plate with depth are demonstrated in Fig. 5. It indicates that the burnt lime treatment make the vertical stress amplitude in the ground fall faster. It also demonstrates that

**Table 2.** Physical and mechanical parameters of burnt-lime-treated soil

Parameter	Value
$Bl_c$ (%)	6
$W_{opt}$ (%)	15
$\rho_{dmax}$ (g/cm <sup>3</sup> )	1.81
$E$ (MPa)	77
$C$ (kPa)	115.4
$\Phi$ (degrees)	34.7

Note:  $Bl_c$  = burnt lime content;  $W_{opt}$  = optimum moisture content;  $\rho_{dmax}$  = maximum dry density;  $E$  = elastic modulus;  $C$  = cohesion; and  $\phi$  = internal friction angle.

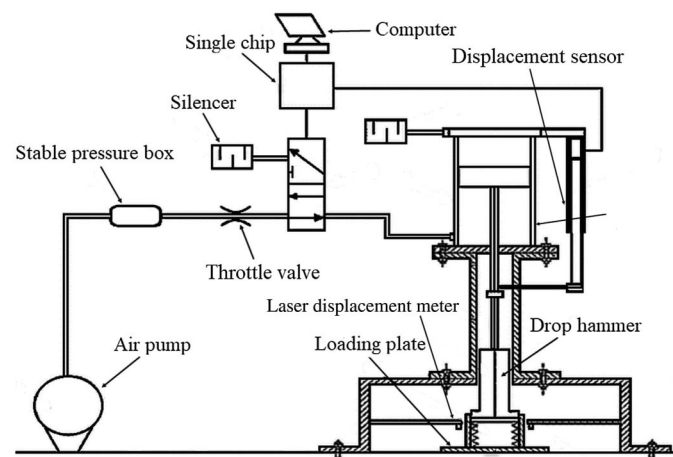


**Fig. 2.** Falling-weight traffic load simulation equipment.

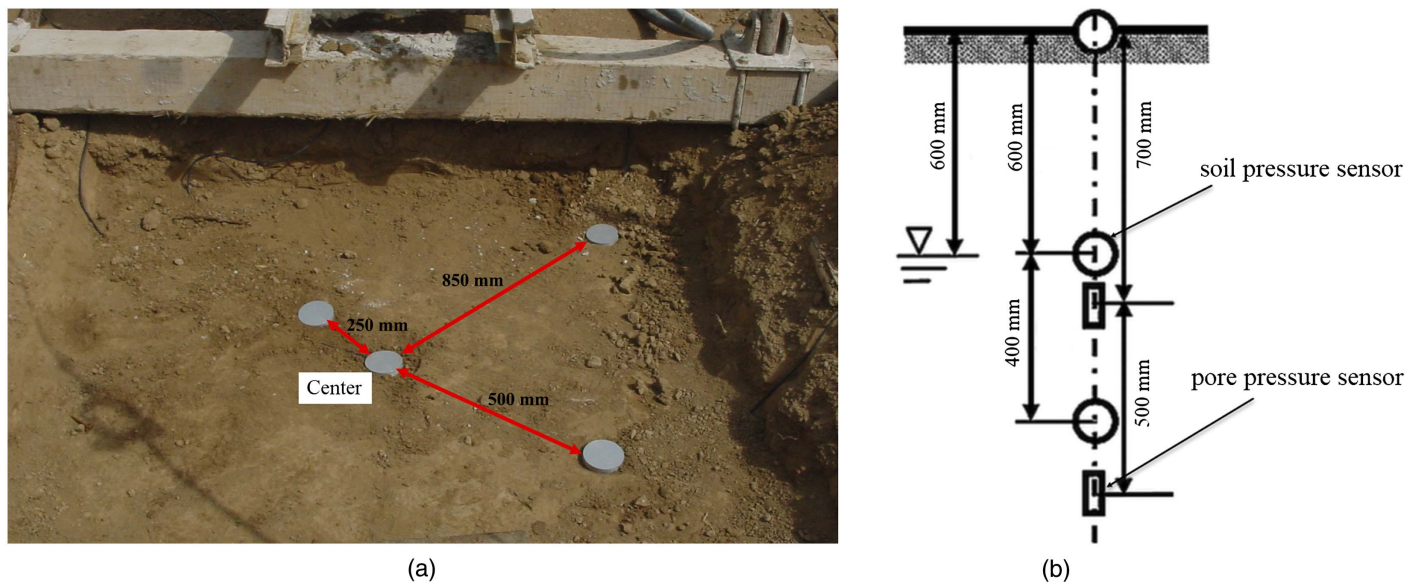


**Fig. 3.** (a) Dynamic soil pressure sensors at the bottom of plate; and (b) Dynamic pore pressure sensors and soil pressure sensors in the soil.

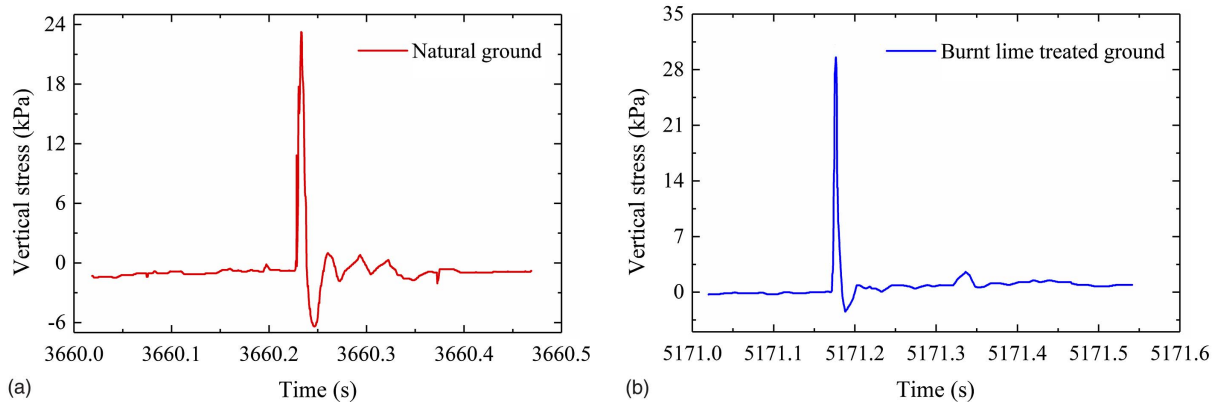


**Fig. 4.** Variation trends of the vertical stress under the center of loading plate: (a) natural ground; and (b) ground treated by burnt lime.

the dynamic stress in the deeper position significantly decreases. Furthermore, this stress decrease in the deeper position can trigger the reduction of the cumulative deformation.

### Excess Pore Water Pressure

The excess pore water pressure in the subsoil can be triggered by repeated traffic loads. Furthermore, the growth of excess pore water pressure can enhance the liquefaction probability of the silt subsoil. As shown in Fig. 6, the growth of the cyclic load number triggers the liquefaction of subsoil, which is manifested by cracking and mud pumping on the ground surface.

During the loading process, the excess pore water pressure changes with the load numbers  $N$ , and these variation trends in the natural and lime-treated ground are shown in Fig. 7. It can be noticed that the excess pore water pressure in the soft substratum that is treated by the burnt lime is significantly lower. This is because the dynamic stress in the substratum is reduced by the lime treatment. (as shown in Fig. 5). Both pore water pressures in the natural and lime-treated ground rapidly increase in the initial loading process. Subsequently, the growth rate of the pore water pressure significantly decreases after a certain load number. Eventually, the pore water pressure remains stable. On the contrary, the pore water

pressure in the natural ground continues to increase, but the growth rate becomes lower. This difference is due to their different drainage conditions. Compared with natural soil, the permeability coefficient of the burnt-lime-treated soil is smaller, and the soil-lime hard crust can block the dissipation of pore water pressure in the substratum. This makes the previously mentioned change trend occur.

Fig. 8 shows the variations of excess pore water pressure after terminating loading. The excess pore water pressure in the lime-treated ground drops sharply at the beginning, and after a brief stabilization it continues to drop to hydrostatic pressure. This variation indicates that the seepage path of water and the dissipation of pore water pressure are both complicated. The pore water pressure of the burnt-lime-treated ground requires a longer dissipation time than that of the natural ground. This is because the hardening of the mud in the lime-soil crust fractures after the end of the cycle, thereby blocking the penetration of water. However, the traffic load is continually present in the actual process, so there is no delay in the dissipation of the pore water pressure.

### Cumulative Settlement

The cumulative deformation caused by traffic load mainly consists of two parts: undrained shear deformation and consolidation

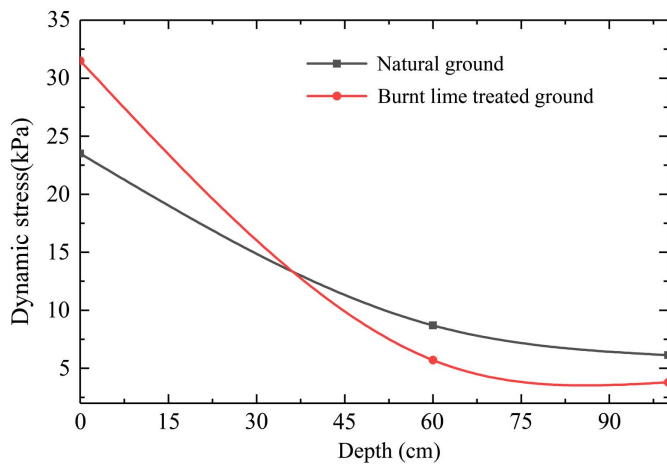
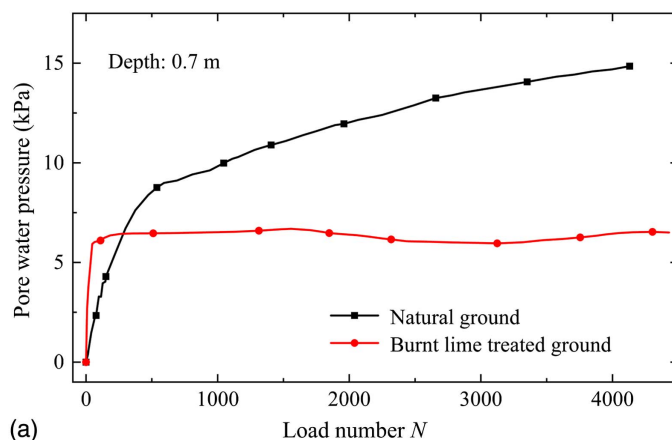


Fig. 5. Vertical stress amplitude at different ground depths.

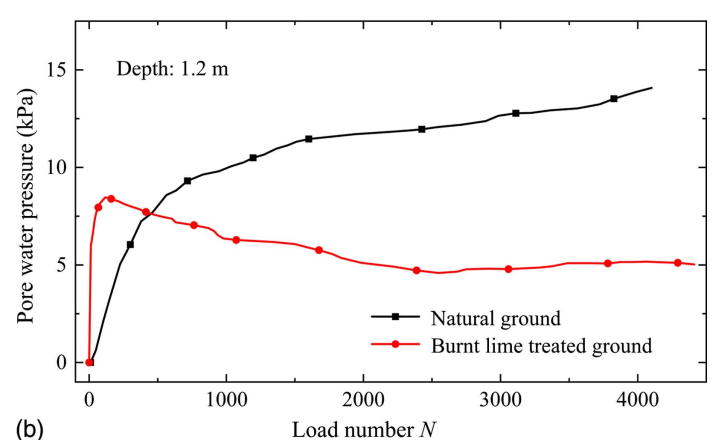


Fig. 6. Mud-pumping phenomenon of the liquefaction ground.

deformation. They both simultaneously appear under actual conditions. However, in the test the co-occurrence of the two exists only in the cycle loading phase. After terminating loading, the consolidation deformation of the soil is the main factor that causes the



(a)



(b)

Fig. 7. Excess pore water pressure under the different load numbers: (a) 0.7 m deep; and (b) 1.2 m deep.

settlement of the subsoil. In the test, the sum of consolidation deformation and undrained shear can be regarded as the total cumulative deformation caused by traffic load (Cui 2012).

Fig. 9 shows the variation curves of the cumulative settlement with the load numbers. The results show that the cumulative settlement growth rate decreases as the load number increases. After burnt lime treatment, the cumulative settlement of the subsoil is significantly reduced. This proves that the burnt lime treatment method for the Yellow River alluvial silt has a mitigating effect on the cumulative settlement caused by traffic load.

Fig. 10 shows the variations of cumulative settlement with time after terminating loading. The cumulative settlement dramatically increases with the dissipation of pore water pressure in a quite short time and eventually becomes stable. Moreover, after terminating loading the cumulative settlement of the natural ground is not much different from that of the burnt-lime-treated ground. However, it took more time for the cumulative settlement of the burnt-lime-treated ground to be stabilized.

### Numerical Simulations of Cumulative Settlement

Numerical methods have advantages in cost and time compared to in situ tests. Therefore, they are often used to simulate the long-term effects of traffic loads. For the cumulative deformation model of soil, a power model was proposed by Monismith et al. (1975) and widely used. Li and Selig (1996) subsequently improved it and proposed the Li-Selig model. Chai and Miura (2002) further refined the Li-Selig model and proposed the Chai-Miura model. The Chai-Miura model considered the role of dynamic deviatoric stress and static strength of soil in cumulative deformation and analyzed the effects of initial static deviatoric stress. Therefore, the Chai-Miura model is widely used to calculate the cumulative deformation of soil.

The Chai-Miura model is demonstrated as follows:

$$\varepsilon_p = a \left( \frac{q_d}{q_f} \right)^m \left( 1 + \frac{q_s}{q_f} \right)^n N^b \quad (1)$$

where  $q_s = \sqrt{3J_{2s}}$  is the initial static deviatoric stress, with  $J_{2s}$  being the second deviatoric stress invariant of initial static stress;  $q_d = \sqrt{3J_{2d}}$  is the dynamic deviatoric stress, with  $J_{2d}$  being the second deviatoric stress invariant of dynamic stress peaks in all directions;  $q_f$  = static strength of soil;  $a$ ,  $b$ ,  $m$ , and  $n$  = parameters of soil; and  $N$  = load numbers.

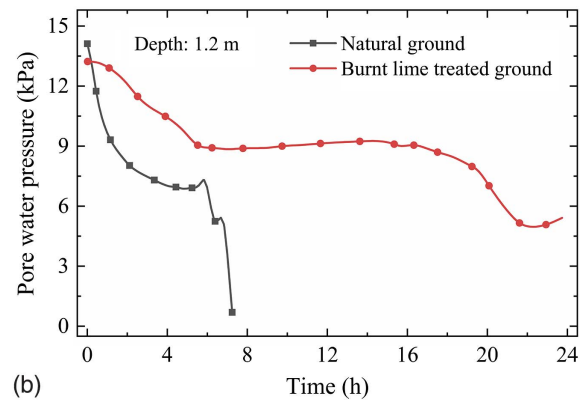
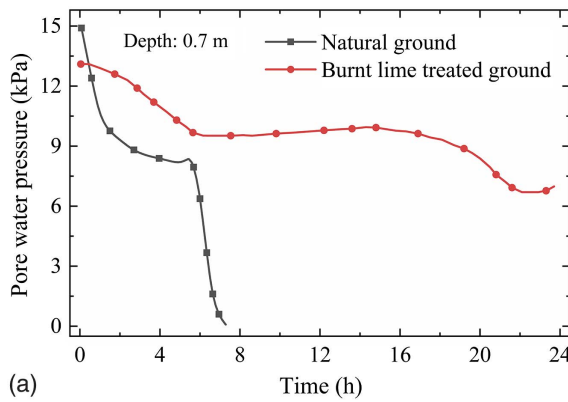


**Fig. 8.** Dissipation of excess pore water pressure after terminating loading: (a) 0.7 m deep; and (b) 1.2 m deep.

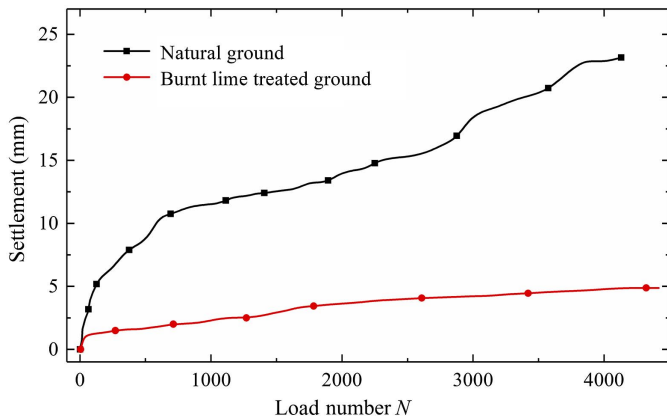


**Fig. 9.** Variation curves of cumulative settlement with loading numbers.

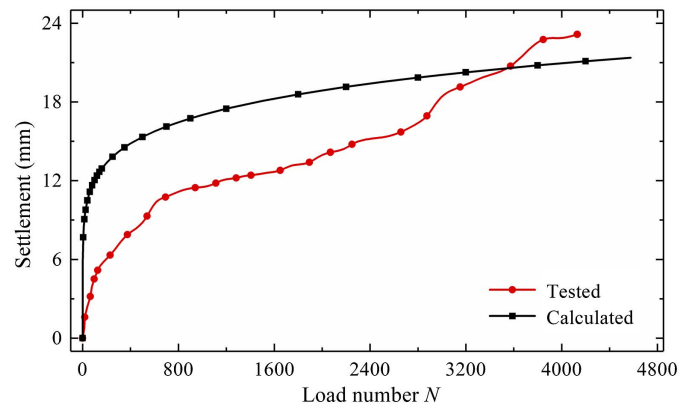


**Fig. 11.** Comparisons between calculated and tested cumulative settlements.

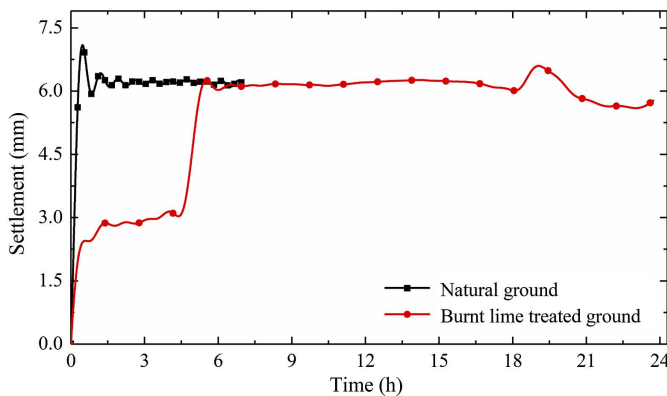


**Fig. 10.** Variation curves of cumulative settlement with time after terminating loading.

According to the effective consolidation stress theory (Shen 2000), the static strength of soil  $q_f$  can be determined by strength index  $c_{cu}$  and  $\phi_{cu}$  of the consolidation undrained total stress

$$q_f = \frac{c_{cu} \cos \phi_{cu}}{1 - \sin \phi_{cu}} + \frac{\frac{1}{2}(1 + K_0)\sigma_{cz} \sin \phi_{cu}}{1 - \sin \phi_{cu}} \quad (2)$$

where  $K_0$  = static soil pressure coefficient at rest; and  $\sigma_{cz}$  = overlying soil pressure.

Variables  $a$ ,  $b$ ,  $m$  and  $n$  in Eq. (1) reflect the combined effect of stress state, physical state, and types of soil. The constants in Eq. (1) were obtained from a series of triaxial tests as  $a = 0.64$ ,  $b = 0.10$ ,  $m = 1.70$ , and  $n = 1.00$ .

### Comparisons and Analyses of the In Situ Test and Numerical Results

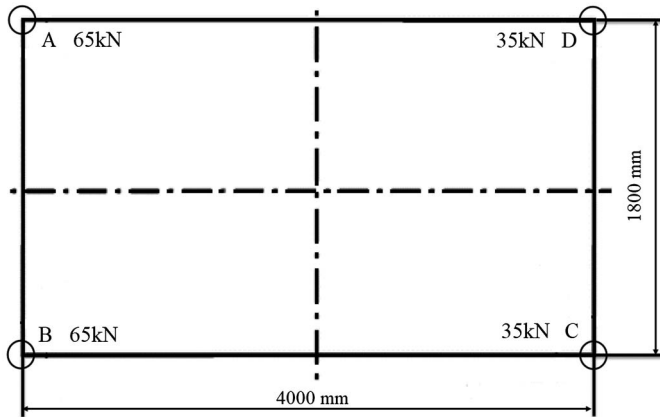
The finite-difference program FLAC3D was used as the calculation tool for the numerical simulation. In order to achieve accurate calculation of the long-term cumulative settlement of subsoil, it is necessary to calculate the cumulative settlement of the natural ground first to determine that the calculation method is valid and feasible.

Primarily, the static module of FLAC3D was used to find the initial static deviatoric stress  $q_s$  in the subsoil. Then the dynamic response of subsoil was determined by the dynamic module of FLAC3D. In the dynamic calculation, the vertical dynamic stresses under the loading plate recorded by soil pressure sensors were loaded on the subsoil surface. The dynamic deviatoric stress  $q_d$  can be determined by the peaks of the dynamic stresses in three orthogonal directions. Finally,  $q_s$  and  $q_d$  were substituted into Eq. (1) and the cumulative deformation of the subsoil can be calculated. The static strength of soil  $q_f$  was calculated by Eq. (2). The cumulative settlement on the subsoil surface can be determined by integrating the vertical cumulative deformation of soil along depth.

The cumulative settlements of the in situ test and the numerical calculation are demonstrated in Fig. 11. The results indicate that

**Table 3.** Road structure and material parameters

Structural layer	Materials	Thickness (cm)	Elastic modulus (MPa)	Poisson's ratio
Upper surface	Stone mastic asphalt	4	1,400	0.3
Middle surface	Mesograin-modified asphalt concrete	6	1,200	0.3
Lower surface	Coarse-graded asphalt concrete	8	1,000	0.3
Upper base	Large grain size asphalt gravel	12	1,400	0.35
Lower base	Cement-stabilized gravel	36	1,500	0.35
Subbase	Lime-ash soil (30% additive gravel)	20	800	0.35
Roadbed	Low liquid limit silt (96% compaction degree)	80	30	0.35
Embankment	Low liquid limit silt (94% compaction degree)	60	17	0.35

**Fig. 12.** Map of Truck-20 load.

the development trends of cumulative settlement obtained by the calculation and the test are roughly the same. Nonetheless, in the initial stage the growth of the calculated settlement is significantly faster. This is mainly triggered by the partial drainage of subsoil during the in situ test. Specifically, the development and dissipation of excess pore water pressure in the subsoil simultaneously occurs during the loading process. However, the Chai-Miura model for numerical simulation was determined by the undrained shear test.

### Numerical Simulations and Analyses of Long-Term Cumulative Settlement

The subsoil of the Xinhe-Xinzhuangzi expressway located in the Yellow River delta was selected to study the long-term settlement. Table 3 gives the material and physical parameters of the expressway.

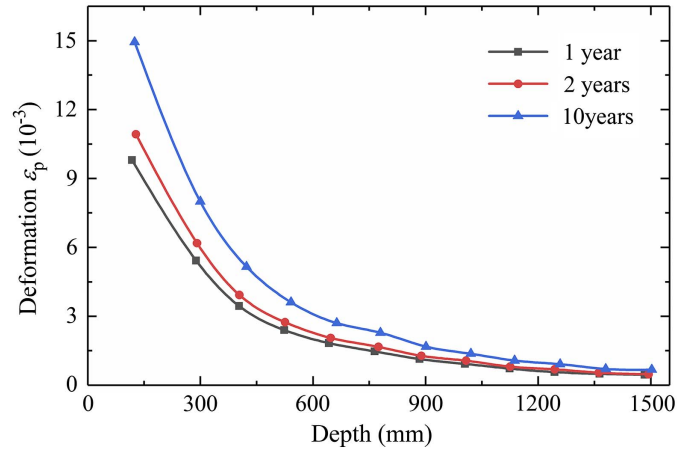
According to the specification JTG D60 (Standards Press of China 2004), the load level of Truck-20 (200-kN live loads) was loaded in the middle of the traffic lane. The weight of the front axles is 70 kN, and that of the rear axles is 130 kN. As shown in Fig. 12, 4-point loads are used to simplify the wheel loads in the calculation. The wheel load is loaded as follows (Huang 1993):

$$F = F_{\max} \sin^2\left(\frac{\pi}{T_s} t\right) \quad 0 \leq t \leq T_s$$

$$F = 0 \quad t > T_s \quad (3)$$

where  $t$  = time;  $F_{\max}$  = wheel load peak, which is 65 kN for the front wheel and 35 kN for the rear wheel; and  $T_s$  = duration of a single vehicle load and has an inverse relationship with the vehicle speed. Herein  $T_s$  is taken as 0.031 s, representing the equivalent vehicle speed of 120 km/h (Huang 1993).

The settlement calculation takes into account changes in the annual traffic volume. Based on the statistical traffic volumes of eight

**Fig. 13.** Variation curves of cumulative deformation with depth.

overpasses along the Xinhe-Xinzhuangzi expressway, the cumulative traffic volumes of the truck can be predicted as follows:

$$N = \frac{73N_1}{\gamma} [(1 + \gamma)^t - 1] \quad (4)$$

where  $N_1$  = 13,463 is the annual average daily traffic at the early stage after opening to traffic;  $\gamma$  = 5.775% is the average annual growth rate; and  $t$  = time in years.

Tables 1–3 give the physical and mechanical parameters of pavement, embankment, and subsoil. The deformation of the soil-lime hard crust was neglected in the calculation and the cumulative deformation of the burnt-lime-treated ground was mainly triggered by the deformation of the natural soil layer. The development trends of cumulative deformation with depth are shown in Fig. 13. It can be seen that about 5 m becomes a clear dividing point. Within 5 m, the cumulative deformation drops extremely fast. After the depth exceeds 5 m, the decrease rate of the cumulative deformation gradually becomes a significantly low level. This implies that the settlement triggered by traffic loads is mainly caused by the cumulative deformation of the silts within 5 m underground.

The development trends of cumulative deformation with time after opening to traffic are shown in Fig. 14. It can be seen that almost 75% of the cumulative settlement is quickly completed in the first year. In the following years, all the settlement gradually completed and eventually stabilized. The cumulative settlement of the natural ground is significantly higher than that of the burnt-lime-treated ground. This suggests that the method of treating the ground with burnt lime has a significant mitigation effect on the cumulative settlement caused by traffic load, which is consistent with the conclusion of the in situ test.

The distribution of cumulative settlement along the road cross section after 10 years of opening to traffic is demonstrated in Fig. 15.

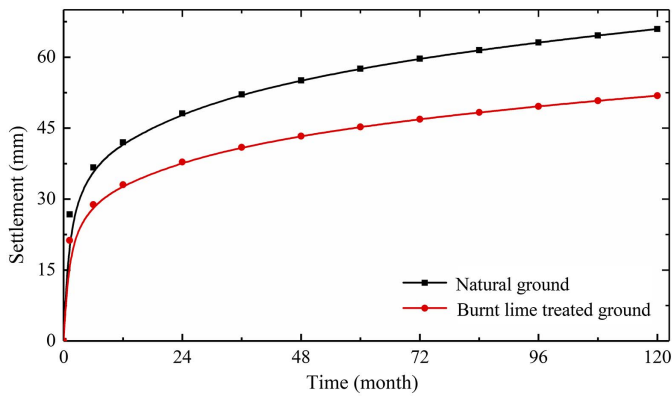


Fig. 14. Variation curves of cumulative settlement with time.

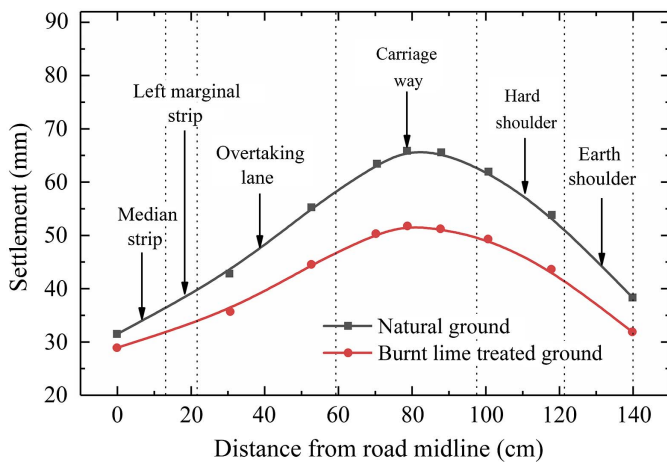


Fig. 15. Transverse distribution curves of cumulative settlement after opening to traffic for 10 years.

It is known that the most serious place of cumulative settlement occurs at the carriageway. Actually, cumulative settlement can trigger a serious reduction in the transverse slope of the road so that the drainage capacity of the road surface is deteriorated. This is not conducive to driving safety and it can also increase the chance of road damage. However, compared to the natural ground, the burnt-lime-treated ground has less settlement at each location on the road. This indicates that treating the alluvial silt ground with burnt lime is an effective method to mitigate the cumulative settlement triggered by traffic load.

## Conclusions

For determining the mitigation effect of burnt lime treatment on the settlement triggered by traffic load, in situ tests and numerical simulations were separately carried out to study the short-term and long-term cumulative sedimentation of the alluvial silt ground. The main conclusions are as follows:

- The burnt-lime-treated ground has higher wave impedance than the natural ground. This causes a significant reduction in the dynamic stress triggered by the traffic load in the substratum. Furthermore, the excess pore water pressure in the substratum of the burnt-lime-treated ground is lower.
- The cumulative settlement of the natural ground is significantly more severe than that of the burnt-lime-treated ground.

This shows that the burnt lime-treated method is an effective way to reduce the cumulative settlement of the alluvial silt ground.

- The burnt-lime-treated method can reduce the probability of road disease triggered by cumulative settlement.

## Data Availability Statement

Some or all data, models, or code generated or used during the study are available from the corresponding author by request.

## Acknowledgments

This work is supported by the National Key R&D Program of China (2018YFB1600100), the Natural Science Foundations of China (Grant Nos. 51778346 and 51479105), and the Key R&D Program of Shandong Province (2017GGX50102).

## References

- Chai, J.-C., and N. Miura. 2002. "Traffic-load-induced permanent deformation of road on soft subsoil." *J. Geotech. Geoenviron.* 128 (11): 907–916. [https://doi.org/10.1061/\(ASCE\)1090-0241\(2002\)128:11\(907\)](https://doi.org/10.1061/(ASCE)1090-0241(2002)128:11(907)).
- Chen, J.-F., and S.-B. Yu. 2011. "Centrifugal and numerical modeling of a reinforced lime-stabilized soil embankment on soft clay with wick drains." *Int. J. Geomech.* 11 (3): 167–173. [https://doi.org/10.1061/\(ASCE\)GM.1943-5622.0000045](https://doi.org/10.1061/(ASCE)GM.1943-5622.0000045).
- Cui, X. Z. 2012. "Traffic-induced settlement of subgrade of low liquid limit silt in Yellow River delta." [In Chinese.] *China Civ. Eng. J.* 45 (1): 154–162.
- Fujiwara, H., and S. Ue. 1990. "Effect of preloading on post-construction consolidation settlement of soft clay subjected to repeated loading." *Soils Found.* 30 (1): 76–86. <https://doi.org/10.3208/sandf1972.30.76>.
- Fujiwara, H., S. Ue, and K. Yasuhara. 1985. "Consolidation of alluvial clay under repeated loading." *Soils Found.* 25 (3): 19–30. [https://doi.org/10.3208/sandf1972.25.3\\_19](https://doi.org/10.3208/sandf1972.25.3_19).
- Heidaripناه, A., M. Nazemi, and F. Soltani. 2016. "Prediction of resilient modulus of lime-treated subgrade soil using different kernels of support vector machine." *Int. J. Geomech.* 17 (2): 06016020. [https://doi.org/10.1061/\(ASCE\)GM.1943-5622.0000723](https://doi.org/10.1061/(ASCE)GM.1943-5622.0000723).
- Huang, Y. H. 1993. *Pavement analysis and design*. Delhi, India: Pearson Education.
- Kamon, M. 1992. "Recent developments of soil improvement." In *Proc., Int. Symp. on Soil Improvement and Pile Foundations I*, 1–16. Nanjing, China: Nanjing University Press.
- Li, D., and E. T. Selig. 1996. "Cumulative plastic deformation for fine-grained subgrade soils." *J. Geotech. Eng.* 122 (12): 1006–1013. [https://doi.org/10.1061/\(ASCE\)0733-9410\(1996\)122:12\(1006\)](https://doi.org/10.1061/(ASCE)0733-9410(1996)122:12(1006)).
- Lu, Z., R. Fang, H. Yao, Z. Hu, and J. Liu. 2018. "Evaluation and analysis of the traffic load-induced settlement of roads on soft subsoils with low embankments." *Int. J. Geomech.* 18 (6): 04018043. [https://doi.org/10.1061/\(ASCE\)GM.1943-5622.0001123](https://doi.org/10.1061/(ASCE)GM.1943-5622.0001123).
- Monismith, C. L., N. Ogawa, and C. R. Freeme. 1975. "Permanent deformation characteristics of subgrade soils due to repeated loading." *Transp. Res. Rec.* 3 (11): 537–554.
- Nash, D., and M. Brown. 2013. "Influence of destructuration of soft clay on time-dependent settlements: Comparison of some elastic viscoplastic models." *Int. J. Geomech.* 15 (5): A4014004. [https://doi.org/10.1061/\(ASCE\)GM.1943-5622.0000281](https://doi.org/10.1061/(ASCE)GM.1943-5622.0000281).
- Seed, H. B., C. K. Chan, and C. L. Monismith. 1955. "Effects of repeated loading on the strength and deformation of compacted clay." In *Proc., Highway Research Board*, 541–558. Washington, DC: Highway Research Board.
- Seed, H. B., and R. L. McNeill. 1956. "Soil deformations in normal compression and repeated loading tests." *Highway Res. Board Bull.* 1 (141): 44–53.



- Shankar, A. R., B. J. Panditharadhy, S. Karishekk, and S. Amulya. 2018. "Experimental investigation of black cotton soil stabilized with lime and coconut coir." In *Proc., Shanghai GeoChina Int. Conf.*, 230–243. New York: Springer.
- Shen, Z. J. 2000. "Earth pressure of clay based on effective consolidation stress theory." [In Chinese.] *Chin. J. Geotech. Eng.* 22 (3): 353–356.
- Standards Press of China. 2004. *General code for design of highway bridges and culverts*. JTJ D60. Beijing: Standards Press of China.
- Wang, X. 2007. "Test on dynamic stress of roadbed and pavement under heavy loads." [In Chinese.] *J. Vib. Shock* 26 (2): 169–173.
- Wei, X., G. Wang, and R. Wu. 2016. "Prediction of traffic loading–induced settlement of low-embankment road on soft subsoil." *Int. J. Geomech.* 17 (2): 06016016. [https://doi.org/10.1061/\(ASCE\)GM.1943-5622.0000719](https://doi.org/10.1061/(ASCE)GM.1943-5622.0000719).
- Yıldırım, H., and H. Erşan. 2007. "Settlements under consecutive series of cyclic loading." *Soil Dyn. Earthquake Eng.* 27 (6): 577–585. <https://doi.org/10.1016/j.soildyn.2006.10.007>.
- Zhang, J., X. Cui, D. Huang, Q. Jin, J. Lou, and W. Tang. 2015. "Numerical simulation of consolidation settlement of pervious concrete pile composite foundation under road embankment." *Int. J. Geomech.* 16 (1): B4015006. [https://doi.org/10.1061/\(ASCE\)GM.1943-5622.0000542](https://doi.org/10.1061/(ASCE)GM.1943-5622.0000542).
- Zhou, Y., Z. Shi, Q. Zhang, and S. Yu. 2018. "Numerical simulation analysis of geogrid-reinforced embankment on soft clay." In *Proc., Shanghai GeoChina Int. Conf.*, 382–389. New York: Springer.
- Zhuang, Y., and X. Cui. 2015. "Case studies of reinforced piled high-speed railway embankment over soft soils." *Int. J. Geomech.* 16 (2): 06015005. [https://doi.org/10.1061/\(ASCE\)GM.1943-5622.0000519](https://doi.org/10.1061/(ASCE)GM.1943-5622.0000519).